How do various forces affect pressure waves in bubbly flows?

Shuya Arai[1] and Tetsuya Kanagawa*[2]

[1]Department of Engineering Mechanics and Energy, Graduate School of Systems and Information and Engineering, University of Tsukuba, Tsukuba 305-8573, Japan
[2]Department of Engineering Mechanics and Energy, Faculty of Engineering, Information and Systems, University of Tsukuba, Tsukuba 305-8573, Japan

Abstract

This study investigated the weak nonlinear propagation of pressure waves in compressible, flowing water with spherical microbubbles, considering various forces. Previous theoretical studies on nonlinear pressure waves in bubbly flows did not consider the forces acting on the bubbles, although the validity of ignoring these forces has not been demonstrated. We considered various forces such as drag, gravity, buoyancy, and Bjerknes forces acting on bubbles and studied their effects on pressure waves in a one-dimensional setting. Using the singular perturbation method, the Korteweg–de Vries–Burgers equation describing wave propagation was derived. The following results were obtained: (i) The Bjerknes force on the bubbles significantly enhanced the nonlinearity, dissipation, and dispersion of the waves. (ii) Drag, gravity, and buoyancy forces increased wave dissipation. (iii) Thermal conduction had the most substantial dissipation effect, followed by acoustic radiation, drag, buoyancy, and gravity. The study confirmed that the attenuation due to forces on gas bubbles is quantitatively minor.

1 Introduction

A pressure wave in a bubbly flow evolves into a shock wave [1, 2, 3] or stable wave (referred to as (acoustic) soliton). These two types of waves display markedly different properties. A shock wave and an acoustic soliton evolve based on the competition between nonlinearity and dissipation and that between nonlinearity and dispersion, respectively. To accurately predict the evolution of a waveform in bubbly flows, it is crucial to understand the relative strengths of three key properties: nonlinearity, dissipation, and dispersion. Extensive research has been conducted on pressure waves in bubbly flows [4, 5, 6, 7, 8, 9, 10, 11] or numerical simulations [12, 13, 14, 15, 16, 17, 18, 19, 20, 21, 22, 23, 24, 25, 26]. However, experiments and numerical analyses alone are insufficient for determining the intricate balance of nonlinearity, dissipation, and dispersion. This gap is effectively filled by theoretical analysis, as highlighted in [27, 28]. Theoretical analysis offers a distinct advantage: it allows for the separate consideration and quantitative evaluation of the factors contributing to wave attenuation, providing a more nuanced and comprehensive understanding of wave dynamics in bubbly flows. The weakly nonlinear (i.e., finite but small amplitude) [29] propagation of pressure waves in bubble flows is described by nonlinear wave equations [30, 31], among which the Korteweg—de Vries—Burgers (KdVB) equation [32, 33, 34, 35] is widely used for low-frequency long waves. The KdVB equation has been proven to align with experimental results in depicting waveforms, as demonstrated in the study by Kuznetsov [36]. This equation is formulated as a linear combination of terms representing nonlinear, dissipation, and dispersion. Therefore, accurately estimating the functions and values of these three key terms is crucial for understanding and predicting the evolution of waveforms in the studied context.

Gas bubbles in a fluid are subject to various forces such as drag [37, 38, 39, 40, 41, 42, 43], lift [44, 45, 46], gravity [47, 48], buoyancy [48, 49], virtual mass force [50], and Bjerknes force [51, 52, 53, 54, 55, 56, 57, 58]. The interaction between these forces and waves in bubbly flows remains underexplored. While previous theoretical studies [32, 33, 34, 35, 36] on nonlinear pressure waves in bubbly flows did not consider the impact of these forces, the lack of investigation into their effects has not been justified.. This oversight may stem from the assumption that these nonoscillatory forces do not influence the oscillatory nature of the waves. Recent studies [59, 60, 61, 62, 63] introduced

*corresponding author: kanagawa.tetsuya.fu@u.tsukuba.ac.jp

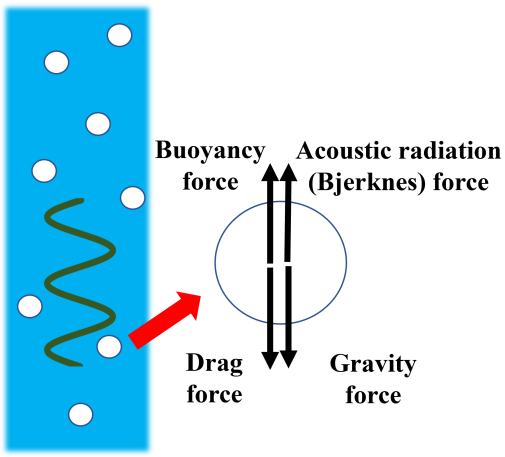

Figure 1: Pressure wave propagation and various forces in bubbly flows.

the drag force into the KdVB equation and showed that the drag force increased wave dissipation. However, the effects of gravity, buoyancy, and Bjerknes forces on waves have not been investigated. In particular, the primary Bjerknes force is the acoustic radiation pressure that is always applied to oscillation bubbles in the propagation of ultrasonic waves [64, 65, 66, 67, 68, 69]. Therefore, this cannot be ignored when dealing with wave theory. Consequently, this study aimed to elucidate the effects of various forces, such as gravity, buoyancy, and Bjerknes forces, on pressure waves in bubbly flows by deriving the KdVB equation. The remainder of this paper is organized as follows. Sec. II introduces the basic equations of the two-fluid model, including drag, gravity, buoyancy, and Bjerknes forces. In Sec. III, we derive the KdVB equation, demonstrating that gravity and buoyancy forces, similar to drag force, enhance wave dissipation. Conversely, the Bjerknes force amplifies nonlinearity, dissipation, and dispersion of the waves. Our numerical analysis indicates that thermal conduction leads in dissipation effect, followed acoustic radiation, drag, buoyancy, and gravity. Sec. IV concludes the paper , highlighting our finding that the attenuation of waves due to forces acting on gas bubbles is relatively minor. This study is the first to validate the practice of disregarding forces in the propagation of pressure waves in bubbly flows.

2 Problem formulation

2.1 Problem statement

We conducted a theoretical investigation of the weak nonlinear (finite but small amplitude) propagation of plane (one-dimensional) progressive pressure waves in flowing compressible water uniformly containing small spherical gas bubbles under various forces, as shown in Fig. 1. The study encompassed a range of forces acting on the bubbles, underpinned by several key assumptions: (i) The motion of the bubbles was assumed to be spherically symmetric. (ii) Bubbles remained stable, without coalescing, breaking, becoming extinct, or forming anew. (iii) In the initial state, both gas and liquid phases flowed at constant velocities. (iv) The temperature of the liquid was considered constant. (v) To simplify the model, direct interactions between bubbles, gas phase viscosity, Reynolds stress, and phase change and mass transport across the bubble-liquid interface were neglected. (vi) The primary Bjerknes force was accounted for, while the secondary Bjerknes force [70, 71, 72, 73, 74] was excluded from consideration.

2.2 Basic equations

To introduce various forces into the interfacial momentum transport, we applied the conservation laws of mass and momentum for the gas and liquid phases based on a two-fluid model [75, 76] as follows:

$$\frac{\partial}{\partial t^*}(\alpha\rho_{\mathrm{G}}^*) + \frac{\partial}{\partial x^*}(\alpha\rho_{\mathrm{G}}^* u_{\mathrm{G}}^*) = 0, \tag{1}$$

$$\frac{\partial}{\partial t^*}[(1-\alpha)\rho_{\mathrm{L}}^*] + \frac{\partial}{\partial x^*}[(1-\alpha)\rho_{\mathrm{L}}^* u_{\mathrm{L}}^*] = 0, \tag{2}$$

$$\frac{\partial}{\partial t^*}(\alpha\rho_{\mathrm{G}}^* u_{\mathrm{G}}^*) + \frac{\partial}{\partial x^*}(\alpha\rho_{\mathrm{G}}^* {u_{\mathrm{G}}^*}^2) + \alpha\frac{\partial p_{\mathrm{G}}^*}{\partial x^*} + 2\mu_{\mathrm{L}}^*\frac{\partial u_{\mathrm{L}}^*}{\partial x^*}\frac{\partial \alpha}{\partial x^*} = F_{\mathrm{vm}}^* + F_{\mathrm{dr}}^* + F_{\mathrm{bje}}^* + F_{\mathrm{buo}}^* + F_{\mathrm{gr,G}}^*, \tag{3}$$

$$\begin{aligned}&\frac{\partial}{\partial t^*}[(1-\alpha)\rho_{\mathrm{L}}^* u_{\mathrm{L}}^*] + \frac{\partial}{\partial x^*}[(1-\alpha)\rho_{\mathrm{L}}^* {u_{\mathrm{L}}^*}^2] + (1-\alpha)\frac{\partial p_{\mathrm{L}}^*}{\partial x^*} + P^*\frac{\partial \alpha}{\partial x^*} - 2\mu_{\mathrm{L}}^*(1-\alpha)\frac{\partial^2 u_{\mathrm{L}}^*}{\partial {x^*}^2}\\ &= -F_{\mathrm{vm}}^* - F_{\mathrm{dr}}^* - F_{\mathrm{bje}}^* - F_{\mathrm{buo}}^* + F_{\mathrm{gr,L}}^*,\end{aligned} \tag{4}$$

where t^* is the time, x^* is the space coordinate normal to the wavefront, α is the void fraction ($0 < \alpha < 1$), μ^* is the viscosity, ρ^* is the density, u^* is the velocity, p^* is the pressure, and P^* is the liquid pressure averaged over bubble–liquid interface [76]. The superscript $*$ denotes a dimensional quantity and the subscripts G and L denote the volume-averaged variables in the gas and liquid phases, respectively.

The following model of virtual mass force [50] is introduced:

$$F_{\mathrm{vm}}^* = -\beta_1\alpha\rho_{\mathrm{L}}^*\left(\frac{\mathrm{D_G}u_{\mathrm{G}}^*}{\mathrm{D}t^*} - \frac{\mathrm{D_L}u_{\mathrm{L}}^*}{\mathrm{D}t^*}\right) - \beta_2\rho_{\mathrm{L}}^*(u_{\mathrm{G}}^* - u_{\mathrm{L}}^*)\frac{\mathrm{D_G}\alpha}{\mathrm{D}t^*} - \beta_3\alpha(u_{\mathrm{G}}^* - u_{\mathrm{L}}^*)\frac{\mathrm{D_G}\rho_{\mathrm{L}}^*}{\mathrm{D}t^*}, \tag{5}$$

where β_1, β_2, and β_3 are constants that can be set as 1/2 for a spherical bubble. The Lagrange derivatives $\mathrm{D_G}/\mathrm{D}t^*$ and $\mathrm{D_L}/\mathrm{D}t^*$ are defined as follows:

$$\frac{\mathrm{D_G}}{\mathrm{D}t^*} = \frac{\partial}{\partial t^*} + u_{\mathrm{G}}^*\frac{\partial}{\partial x^*}, \quad \frac{\mathrm{D_L}}{\mathrm{D}t^*} = \frac{\partial}{\partial t^*} + u_{\mathrm{L}}^*\frac{\partial}{\partial x^*}. \tag{6}$$

We introduce a model for the drag force term F_{dr}^* for spherical bubbles [59]:

$$F_{\mathrm{dr}}^* = -\frac{3}{8R^*}\alpha C_{\mathrm{D}}\rho_{\mathrm{L}}^*(u_{\mathrm{G}}^* - u_{\mathrm{L}}^*)|u_{\mathrm{G}}^* - u_{\mathrm{L}}^*|, \tag{7}$$

where R^* is the representative bubble radius and C_{D} is the drag coefficient for a single spherical bubble.

We introduce the gravity, buoyancy, and Bjerknes forces [48, 49] as follows:

$$F_{\mathrm{gr,G}}^* = -\alpha\rho_G^* g^*, \quad F_{\mathrm{gr,L}}^* = -(1-\alpha)\rho_L^* g^*, \tag{8}$$

$$F_{\mathrm{buo}}^* = \alpha\rho_L^* g^*, \tag{9}$$

$$F_{\mathrm{bje}}^* = -B\alpha\frac{\partial p_L^*}{\partial x^*}, \tag{10}$$

where g^* is acceleration due to gravity and B is a constant. We use B to verify the effect of Bjerknes force. Here, $B = 0$ and $B = 1$ correspond to the cases of without and with Bjerknes force, respectively.

We employed the equation of motion for the bubbles, formulated as a linear combination of their volumetric oscillations [77] and translation movements [78, 79, 80]. This approach integrates the dynamics of bubble oscillation and translation to comprehensively describe their motion:

$$\begin{aligned}&\left(1 - \frac{1}{c_{\mathrm{L0}}^*}\frac{\mathrm{D_G}R^*}{\mathrm{D}t^*}\right)R^*\frac{\mathrm{D_G^2}R^*}{\mathrm{D}{t^*}^2} + \frac{3}{2}\left(1 - \frac{1}{3c_{\mathrm{L0}}^*}\frac{\mathrm{D_G}R^*}{\mathrm{D}t^*}\right)\left(\frac{\mathrm{D_G}R^*}{\mathrm{D}t^*}\right)^2\\ &= \left(1 + \frac{1}{c_{\mathrm{L0}}^*}\frac{\mathrm{D_G}R^*}{\mathrm{D}t^*}\right)\frac{P^*}{\rho_{\mathrm{L0}}^*} + \frac{R^*}{\rho_{\mathrm{L0}}^* c_{\mathrm{L0}}^*}\frac{\mathrm{D_G}}{\mathrm{D}t^*}(p_{\mathrm{L}}^* + P^*) + \frac{(u_{\mathrm{G}}^* - u_{\mathrm{L}}^*)^2}{4},\end{aligned} \tag{11}$$

where c_{L0}^* is the speed of sound in pure water.

In our study, we incorporated the energy equation [81] for thermal conduction at the bubble–liquid interface To account for the thermal effects within the bubble.

$$\frac{\mathrm{D_G}p_{\mathrm{G}}^*}{\mathrm{D}t^*} = \frac{3}{R^*}\left[(\kappa-1)\lambda_{\mathrm{G}}^*\left.\frac{\partial T_{\mathrm{G}}^*}{\partial r^*}\right|_{r^*=R^*} - \kappa p_{\mathrm{G}}^*\frac{\mathrm{D_G}R^*}{\mathrm{D}t^*}\right], \tag{12}$$

where T^*_{G} is the gas temperature, κ is the specific heat ratio, r^* is the radial distance from the center of the bubble and λ^*_{G} is the thermal conductivity of the gas inside the bubble. A previous study [81] did not use a temperature-gradient model. However, certain models for the temperature-gradient as the first term on the right-hand side of (12) were proposed. This study used the model proposed by Sugiyama et al. [82]:

$$\left.\frac{\partial T^*_{\mathrm{G}}}{\partial r^*}\right|_{r^*=R^*} = \frac{\mathrm{Re}(\widetilde{L^*_{\mathrm{p}}})(T^*_{\mathrm{G0}} - T^*_{\mathrm{G}})}{|\widetilde{L^*_{\mathrm{p}}}|^2} + \frac{\mathrm{Im}(\widetilde{L^*_{\mathrm{p}}})}{\omega^*_{\mathrm{B}}|\widetilde{L^*_{\mathrm{p}}}|^2}\frac{\mathrm{D_G}T^*_{\mathrm{G}}}{\mathrm{D}t^*}, \tag{13}$$

where Re and Im are the real and imaginary parts, respectively. The physical quantities in the initial state are denoted by the subscript 0 and are constants. Certain symbols are defined as follows [82]:

$$\omega^*_{\mathrm{B}} = \sqrt{\frac{3\gamma_{\mathrm{e}}(p^*_{\mathrm{L0}} + 2\sigma^*/R^*_0) - 2\sigma^*/R^*_0}{\rho^*_{\mathrm{L0}}R^{*2}_0} - \left(\frac{2\mu^*_{\mathrm{e0}}}{\rho^*_{\mathrm{L0}}R^{*2}_0}\right)^2}, \tag{14}$$

$$\gamma_{\mathrm{e}} = \mathrm{Re}\left(\frac{\Gamma_{\mathrm{N}}}{3}\right), \tag{15}$$

$$\mu^*_{\mathrm{e0}} = \mu^*_{\mathrm{L}} + \mathrm{Im}\left(\frac{p^*_{\mathrm{G0}}\Gamma_{\mathrm{N}}}{4\omega^*_{\mathrm{B}}}\right), \tag{16}$$

$$\Gamma_{\mathrm{N}} = \frac{3\alpha^2_{\mathrm{N}}\kappa}{\alpha^2_{\mathrm{N}} + 3(\kappa-1)(\alpha_{\mathrm{N}}\coth\alpha_{\mathrm{N}} - 1)}, \tag{17}$$

$$\alpha_{\mathrm{N}} = \sqrt{\frac{\kappa\omega^*_{\mathrm{B}}p^*_{\mathrm{G0}}R^{*2}_0}{2(\kappa-1)T^*_{\mathrm{G0}}\lambda^*_{\mathrm{G}}}}(1+\mathrm{i}), \tag{18}$$

$$\widetilde{L^*_{\mathrm{p}}} = \frac{R^*_0(\alpha^2_{\mathrm{N}} - 3\alpha_{\mathrm{N}}\coth\alpha_{\mathrm{N}} + 3)}{\alpha^2_{\mathrm{N}}(\alpha_{\mathrm{N}}\coth\alpha_{\mathrm{N}} - 1)}, \tag{19}$$

where ω^*_{B} is the eigenfrequency of a single bubble, γ_{e} is the effective polytropic exponent, μ^*_{e0} is the initial effective viscosity, σ^* is the surface tension, i denotes an imaginary unit, and Γ_{N}, α_{N}, and $\widetilde{L^*_{\mathrm{p}}}$ are complex numbers.

To complete the set of (1)–(4), (11), and (12), the equation of state for an ideal gas, the Tait equation of state for liquid, mass conservation law of the gas inside the bubbles, and balance of normal stresses across the bubble–liquid interface are introduced as follows:

$$\frac{p^*_{\mathrm{G}}}{p^*_{\mathrm{G0}}} = \frac{\rho^*_{\mathrm{G}}}{\rho^*_{\mathrm{G0}}}\frac{T^*_{\mathrm{G}}}{T^*_{\mathrm{G0}}}, \tag{20}$$

$$p^*_{\mathrm{L}} = p^*_{\mathrm{L0}} + \frac{\rho^*_{\mathrm{L0}}{c^*_{\mathrm{L0}}}^2}{n}\left[\left(\frac{\rho^*_{\mathrm{L}}}{\rho^*_{\mathrm{L0}}}\right)^n - 1\right], \tag{21}$$

$$\frac{\rho^*_{\mathrm{G}}}{\rho^*_{\mathrm{G0}}} = \left(\frac{R^*_0}{R^*}\right)^3, \tag{22}$$

$$p^*_{\mathrm{G}} - (p^*_{\mathrm{L}} + P^*) = \frac{2\sigma^*}{R^*} + \frac{4\mu^*_{\mathrm{L}}}{R^*}\frac{\mathrm{D_G}R^*}{\mathrm{D}t^*}, \tag{23}$$

where n is a material constant (e.g., $n = 7.15$ for water).

2.3 Analysis on multiple scales

Using the method of multiple scales [31], we introduce four scales as extended independent variables. This approach is based on the assumption of a finite but small nondimensional wave amplitude, denoted as $\epsilon(\ll 1)$:

$$t_0 = t, \quad t_1 = \epsilon t; \quad x_0 = x, \quad x_1 = \epsilon x, \tag{24}$$

where the nondimensional independent variables are defined by $t = t^*/T^*$ and $x = x^*/L^*$, T^* is the typical period and L^* is a typical wavelength. Here, the subscripts 0 and 1 correspond to the near and far field [31]. For example, t_0 is the nondimensional time for the near field. Note that the difference between the constant denoted by subscript 0 and near field by 0.

The dependent variables are nondimensionalized and expanded in the power series of ϵ as follows:

$$R^*/R_0^* = 1 + \epsilon R_1 + \epsilon^2 R_2 + O(\epsilon^3), \tag{25}$$

$$u_{\mathrm{G}}^*/U^* = u_{\mathrm{G}0} + \epsilon u_{\mathrm{G}1} + \epsilon^2 u_{\mathrm{G}2} + O(\epsilon^3), \tag{26}$$

$$u_{\mathrm{L}}^*/U^* = u_{\mathrm{L}0} + \epsilon u_{\mathrm{L}1} + \epsilon^2 u_{\mathrm{L}2} + O(\epsilon^3), \tag{27}$$

$$\alpha/\alpha_0 = 1 + \epsilon\alpha_1 + \epsilon^2\alpha_2 + O(\epsilon^3), \tag{28}$$

$$\rho_{\mathrm{L}}^*/\rho_{\mathrm{L}0}^* = 1 + \epsilon^2\rho_{\mathrm{L}1} + O(\epsilon^3), \tag{29}$$

$$p_{\mathrm{L}}^*/(\rho_{\mathrm{L}0}^* U^{*2}) = p_{\mathrm{L}0} + \epsilon p_{\mathrm{L}1} + \epsilon^2 p_{\mathrm{L}2} + O(\epsilon^3), \tag{30}$$

$$T_{\mathrm{G}}^*/T_{\mathrm{G}0}^* = 1 + \epsilon T_{\mathrm{G}1} + \epsilon^2 T_{\mathrm{G}2} + O(\epsilon^3), \tag{31}$$

where $U^* (\equiv L^*/T^*)$ is the typical propagation speed, and the initial nondimensional pressure $p_{\mathrm{G}0}$ and $p_{\mathrm{L}0}$ are defined as $p_{\mathrm{G}0} \equiv p_{\mathrm{G}0}^*/(\rho_{\mathrm{L}0}^* U^{*2}) \equiv O(1)$ and $p_{\mathrm{L}0} \equiv p_{\mathrm{L}0}^*/(\rho_{\mathrm{L}0}^* U^{*2}) \equiv O(1)$, Furthermore, the ratio of the initial densities of the gas and liquid phases is sufficiently small.

As the scaling relations of nondimensional ratios are derived using ϵ, the low-frequency long wave is described by the following ratios:

$$\frac{U^*}{c_{\mathrm{L}0}^*} \equiv O(\sqrt{\epsilon}) \equiv V\sqrt{\epsilon}, \tag{32}$$

$$\frac{R_0^*}{L^*} \equiv O(\sqrt{\epsilon}) \equiv \Delta\sqrt{\epsilon}, \tag{33}$$

$$\frac{\omega^*}{\omega_{\mathrm{B}}^*} \equiv \frac{1}{T^*\omega_{\mathrm{B}}^*} \equiv O(\sqrt{\epsilon}) \equiv \Omega\sqrt{\epsilon}, \tag{34}$$

where V, Δ, and Ω are the constants of $O(1)$. Equations (32)–(34) provide critical insights into the acoustic properties of bubbly flows. They demonstrate that the speed of sound within these flows is significantly lower compared to that in pure water. Additionally, the initial radius of the bubbles is markedly smaller than a typical wavelength observed in such environments. Furthermore, the incident frequency of waves within bubbly flows is substantially lower than the eigenfrequency of individual bubbles.

We determined the sizes of the nondimensional numbers for the thermal effect [61, 63]:

$$\frac{3(\kappa-1)\lambda_{\mathrm{G}}^*}{p_{\mathrm{G}0}^*\omega^* R_0^*}\frac{\mathrm{Re}(\widetilde{L_{\mathrm{p}}^*})T_{\mathrm{G}0}^*}{|\widetilde{L_{\mathrm{p}}^*}|^2} = \zeta_{\mathrm{STM}1}\epsilon, \quad \frac{3(\kappa-1)\lambda_{\mathrm{G}}^*}{p_{\mathrm{G}0}^*\omega^* R_0^*}\frac{\omega^*\mathrm{Im}(\widetilde{L_{\mathrm{p}}^*})T_{\mathrm{G}0}^*}{\omega_{\mathrm{B}}^*|\widetilde{L_{\mathrm{p}}^*}|^2} = \zeta_{\mathrm{STM}2}\epsilon^2. \tag{35}$$

The scaling relation of the acceleration owing to gravity g^* is

$$\frac{T^* g^*}{U^*} = g\epsilon, \tag{36}$$

where g is a constant of $O(1)$.

The scaling relation of the liquid viscosity μ_{L}^* is

$$\frac{\mu_{\mathrm{L}}^*}{\rho_{\mathrm{L}0}^* U^* L^*} \equiv O(\epsilon^2) \equiv \mu_{\mathrm{L}}\epsilon^2, \tag{37}$$

where μ_{L} is a constant of $O(1)$.

The drag coefficient C_{D} is defined as follows:

$$C_{\mathrm{D}} \equiv \frac{A\mu_{\mathrm{L}}^*}{|u_{\mathrm{G}}^* - u_{\mathrm{L}}^*|\rho_{\mathrm{L}}^* 2R^*}, \tag{38}$$

where A is a constant (e.g., $A = 16$), and C_{D} depends on Reynolds number Re ($C_{\mathrm{D}} = A/\mathrm{Re}$) [83].

3 Results

3.1 Linear propagation at near field

By substituting (24)–(38) into (1)–(4), (11), and (12), we obtain a set of linear equations using (20)–(23) from the leading-order approximation:

$$\frac{\mathrm{D}\alpha_1}{\mathrm{D}t_0} - 3\frac{\mathrm{D}R_1}{\mathrm{D}t_0} + \frac{\partial u_{\mathrm{G1}}}{\partial x_0} = 0, \tag{39}$$

$$\alpha_0\frac{\mathrm{D}\alpha_1}{\mathrm{D}t_0} - (1-\alpha_0)\frac{\partial u_{\mathrm{L1}}}{\partial x_0} = 0, \tag{40}$$

$$\beta_1\left(\frac{\mathrm{D}u_{\mathrm{G1}}}{\mathrm{D}t_0} - \frac{\mathrm{D}u_{\mathrm{L1}}}{\mathrm{D}t_0}\right) - 3p_{\mathrm{G0}}\frac{\partial R_1}{\partial x_0} + p_{\mathrm{G0}}\frac{\partial T_{\mathrm{G1}}}{\partial x_0} + B\frac{\partial p_{\mathrm{L1}}}{\partial x_0} = 0, \tag{41}$$

$$(1-\alpha_0)\frac{\mathrm{D}u_{\mathrm{L1}}}{\mathrm{D}t_0} - \alpha_0\beta_1\left(\frac{\mathrm{D}u_{\mathrm{G1}}}{\mathrm{D}t_0} - \frac{\mathrm{D}u_{\mathrm{L1}}}{\mathrm{D}t_0}\right) - \alpha_0 u_0\frac{\mathrm{D}\alpha_1}{\mathrm{D}t_0} + u_0(1-\alpha_0)\frac{\partial u_{\mathrm{L1}}}{\partial x_0} + (1-\alpha_0)\frac{\partial p_{\mathrm{L1}}}{\partial x_0} - \alpha_0 B\frac{\partial p_{\mathrm{L1}}}{\partial x_0} = 0, \tag{42}$$

$$\left[3(\gamma_{\mathrm{e}}-1)p_{\mathrm{G0}} - \frac{\Delta^2}{\Omega^2}\right]R_1 + p_{\mathrm{G0}}T_{\mathrm{G1}} - p_{\mathrm{L1}} = 0, \tag{43}$$

$$\frac{\mathrm{D}T_{\mathrm{G1}}}{\mathrm{D}t_0} + 3(\kappa-1)\frac{\mathrm{D}R_1}{\mathrm{D}t_0} = 0. \tag{44}$$

Although gravitational and buoyancy forces do not appear here, the effect of Bjerknes force ($F^*_{\mathrm{bje}} = -B\alpha\partial p^*_L/\partial x^*$) is described by the last term on the left side of (41) and (42).

Combining (39) and (44) results in a linear wave equation for the first-order variation in bubble radius R_1:

$$\frac{\mathrm{D}^2R_1}{\mathrm{D}t_0^2} - v_{\mathrm{p}}^2\frac{\partial^2 R_1}{\partial x_0^2} = 0, \tag{45}$$

where v_{p} is the phase velocity expressed as

$$v_p = \sqrt{\frac{\alpha_0\kappa(1-\alpha_0+\beta_1) - (\beta_1+\alpha_0 B)(1-\alpha_0)(\gamma_e-\kappa)}{\alpha_0\beta_1(1-\alpha_0)}p_{G0} + \frac{\beta_1+\alpha_0 B}{3\alpha_0\beta_1}\frac{\Delta^2}{\Omega^2}}. \tag{46}$$

The linear Lagrange derivative $\mathrm{D}/\mathrm{D}t_0$ is defined as

$$\frac{\mathrm{D}}{\mathrm{D}t_0} = \frac{\partial}{\partial t_0} + u_0\frac{\partial}{\partial x_0}. \tag{47}$$

For simplicity, the initial velocities of both phases are assumed to be the same ($u_{\mathrm{G0}} = u_{\mathrm{L0}} \equiv u_0$). However, the perturbations of the velocities are not the same ($u_{\mathrm{G1}} \neq u_{\mathrm{L1}}$). Setting $v_{\mathrm{p}} = 1$ yields the explicit form of U^* as

$$U^* = \sqrt{\frac{\alpha_0\kappa(1-\alpha_0+\beta_1) - (\beta_1+\alpha_0 B)(1-\alpha_0)(\gamma_e-\kappa)}{\alpha_0\beta_1(1-\alpha_0)}\frac{p^*_{G0}}{\rho^*_{L0}} + \frac{\beta_1+\alpha_0 B}{3\alpha_0\beta_1}R_0^{*2}\omega_B^{*2}}. \tag{48}$$

Value of the typical propagation speed U^* is increased by considering Bjerknes force, as shown in Table 1.

By focusing on the right-running wave (i.e., by introducing the moving coordinates $\varphi_0 = x_0 - v_{\mathrm{p}}t_0$), α_1, u_{G1}, u_{L1}, p_{L1}, and T_{G1} are expressed in terms of R_1.

$$\alpha_1 = s_1R_1, \quad u_{\mathrm{G1}} = s_2R_1, \quad u_{\mathrm{L1}} = s_3R_1, \quad p_{\mathrm{L1}} = s_4R_1, \quad T_{\mathrm{G1}} = s_5R_1 \tag{49}$$

with

$$s_1 = \frac{(1-\alpha_0)}{\alpha_0(1-\alpha_0+\beta_1)}\left[3\alpha_0\beta_1 - \frac{(1-\alpha_0-\alpha_0 B)s_4}{v_p^2}\right], \quad s_2 = v_p(s_1-3),$$
$$s_3 = -v_p\frac{\alpha_0}{1-\alpha_0}s_1, \quad s_4 = 3p_{G0}(\gamma_e-\kappa) - \frac{\Delta^2}{\Omega^2}, \quad s_5 = -3(\kappa-1). \tag{50}$$

Note that s_1, s_2, and s_3 change due to the effects of Bjerknes force, whereas s_4 and s_5 do not change.

Table 1: Value of Typical propagation speed U^*

R_0^*	α_0	$U^*\|_{B=0}$ [m/s]	$(U^*\|_{B=1}$ - $U^*\|_{B=0})$ / $U^*\|_{B=0}$
5mm	0.0001 (0.01%)	1.2×10^3	0.010
	0.001 (0.1%)	3.8×10^2	0.10
	0.01 (1%)	1.2×10^2	0.97
500μm	0.0001 (0.01%)	1.2×10^3	0.010
	0.001 (0.1%)	3.8×10^2	0.10
	0.01 (1%)	1.2×10^2	0.97
50μm	0.0001 (0.01%)	1.2×10^3	0.010
	0.001 (0.1%)	3.8×10^2	0.10
	0.01 (1%)	1.2×10^2	0.97

3.2 Nonlinear propagation at far field

As in the case of $O(\epsilon)$, the following set of inhomogeneous equations for $O(\epsilon^2)$ is derived:

$$\frac{\mathrm{D}\alpha_2}{\mathrm{D}t_0} - 3\frac{\mathrm{D}R_2}{\mathrm{D}t_0} + \frac{\partial u_{\mathrm{G}2}}{\partial x_0} = K_1, \tag{51}$$

$$\alpha_0\frac{\mathrm{D}\alpha_2}{\mathrm{D}t_0} - (1-\alpha_0)\frac{\partial u_{\mathrm{L}2}}{\partial x_0} = K_2, \tag{52}$$

$$\beta_1\left(\frac{\mathrm{D}u_{\mathrm{G}2}}{\mathrm{D}t_0} - \frac{\mathrm{D}u_{\mathrm{L}2}}{\mathrm{D}t_0}\right) - 3p_{\mathrm{G}0}\frac{\partial R_2}{\partial x_0} + p_{\mathrm{G}0}\frac{\partial T_{\mathrm{G}2}}{\partial x_0} + B\frac{\partial p_{\mathrm{L}2}}{\partial x_0} = K_3, \tag{53}$$

$$(1-\alpha_0)\frac{\mathrm{D}u_{\mathrm{L}2}}{\mathrm{D}t_0} - \alpha_0\beta_1\left(\frac{\mathrm{D}u_{\mathrm{G}2}}{\mathrm{D}t_0} - \frac{\mathrm{D}u_{\mathrm{L}2}}{\mathrm{D}t_0}\right) - \alpha_0 u_0\frac{\mathrm{D}\alpha_2}{\mathrm{D}t_0} + u_0(1-\alpha_0)\frac{\partial u_{\mathrm{L}2}}{\partial x_0} + (1-\alpha_0)\frac{\partial p_{\mathrm{L}2}}{\partial x_0} - \alpha_0 B\frac{\partial p_{\mathrm{L}2}}{\partial x_0} = K_4, \tag{54}$$

$$\left[3(\gamma_{\mathrm{e}}-1)p_{\mathrm{G}0} - \frac{\Delta^2}{\Omega^2}\right]R_2 + p_{\mathrm{G}0}T_{\mathrm{G}2} - p_{\mathrm{L}2} = K_5, \tag{55}$$

$$\frac{\mathrm{D}T_{\mathrm{G}2}}{\mathrm{D}t_0} + 3(\kappa-1)\frac{\mathrm{D}R_2}{\mathrm{D}t_0} = K_6, \tag{56}$$

where the inhomogeneous terms K_i $(1 \le i \le 6)$ are explicitly presented in the Appendix.

Consequently, (51)–(56) are combined into a single inhomogeneous equation:

$$\frac{\mathrm{D}^2 R_2}{\mathrm{D}t_0^2} - v_{\mathrm{p}}^2\frac{\partial^2 R_2}{\partial x_0^2} = K, \tag{57}$$

where

$$\begin{aligned} K = &-\frac{1}{3}\frac{DK_1}{Dt_0} + \frac{1}{3\alpha_0}\frac{DK_2}{Dt_0} + \frac{u_0}{3\alpha_0(1-\alpha_0)}\frac{\partial K_2}{\partial x_0} + \frac{1-\alpha_0+\beta_1}{3(1-\alpha_0)\beta_1}\frac{\partial K_3}{\partial x_0} \\ &+ \frac{1}{3\alpha_0(1-\alpha_0)}\frac{\partial K_4}{\partial x_0} + \frac{\beta_1+\alpha_0 B}{3\alpha_0\beta_1}\frac{\partial^2 K_5}{\partial x_0^2} - \frac{p_{G0}[\alpha_0(1-\alpha_0)+\beta_1+\alpha_0 B(1-\alpha_0)]}{3\alpha_0\beta_1(1-\alpha_0)}\int\frac{\partial^2 K_6}{\partial {x_0}^2}dt_0. \end{aligned} \tag{58}$$

Based on the solvability condition for (57), $K = 0$ is required [31]. From (24), the original independent variables x and t are restored.

$$\frac{\partial f}{\partial t} + (u_0 + v_{\mathrm{p}})\frac{\partial f}{\partial x} + \epsilon\left(\Pi_0\frac{\partial f}{\partial x} + \Pi_1 f\frac{\partial f}{\partial x} + \Pi_2\frac{\partial^2 f}{\partial x^2} + \Pi_3\frac{\partial^3 f}{\partial x^3} + \Pi_4 f\right) = 0. \tag{59}$$

Finally, we obtain the KdVB equation:

$$\frac{\partial f}{\partial \tau} + \Pi_1 f\frac{\partial f}{\partial \xi} + \Pi_2\frac{\partial^2 f}{\partial \xi^2} + \Pi_3\frac{\partial^3 f}{\partial \xi^3} + \Pi_4 f = 0, \tag{60}$$

using a variable transform

$$\tau = \epsilon t, \quad \xi = x - (u_0 + v_{\mathrm{p}} + \epsilon\Pi_0)t, \tag{61}$$

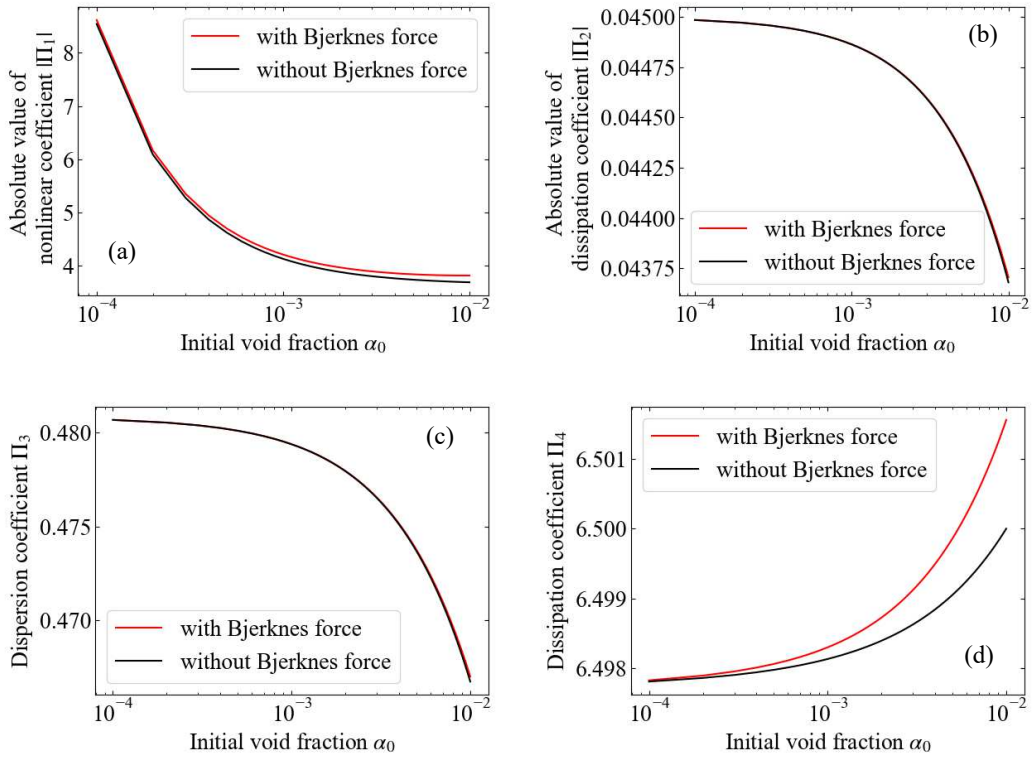

Figure 2: (a) Absolute value of nonlinear coefficient $|\Pi_1|$, (b) absolute value of dissipation coefficient owing to acoustic radiation $|\Pi_2|$ (Table 2), (c) Dispersion coefficient Π_3 (Table 3), and (d) Dissipation coefficient Π_4 as a function of the initial void fraction α_0. The calculation condition is $R_0^* = 500\mu\mathrm{m}$, $\sqrt{\epsilon} = 0.15$, $p_{\mathrm{L}0}^* = 101325\mathrm{Pa}$, $\rho_{\mathrm{L}0}^* = 1000\mathrm{kg/m^3}$, $\sigma^* = 0.0728\mathrm{N/m}$, $c_{\mathrm{L}0}^* = 1500\mathrm{m/s}$, $\mu_{\mathrm{L}}^* = 10^{-3}\mathrm{Pa\cdot s}$, $u_0 = 1$, and $v_{\mathrm{p}} = 1$.

Table 2: Absolute value of dissipation coefficient $|\Pi_2|$ in Fig. 2.

R_0^*	α_0	$\lvert\Pi_2\rvert\rvert_{B=0}$	($\lvert\Pi_2\rvert\rvert_{B=1}$ - $\lvert\Pi_2\rvert\rvert_{B=0}$) / $\lvert\Pi_2\rvert\rvert_{B=0}$
5mm	0.0001 (0.01%)	4.6×10^{-2}	6.0×10^{-6}
	0.001 (0.1%)	4.5×10^{-2}	6.0×10^{-4}
	0.01 (1%)	4.4×10^{-2}	5.7×10^{-2}
500μm	0.0001 (0.01%)	4.5×10^{-2}	6.0×10^{-6}
	0.001 (0.1%)	4.5×10^{-2}	6.0×10^{-4}
	0.01 (1%)	4.4×10^{-2}	5.7×10^{-2}
50μm	0.0001 (0.01%)	4.3×10^{-2}	6.0×10^{-6}
	0.001 (0.1%)	4.3×10^{-2}	6.0×10^{-4}
	0.01 (1%)	4.2×10^{-2}	5.8×10^{-2}

Table 3: Value of dispersion coefficient Π_3 in Fig. 2.

R_0^*	α_0	$\Pi_3\|_{B=0}$	$(\Pi_3\|_{B=1}$ - $\Pi_3\|_{B=0})$ / $\Pi_3\|_{B=0}$
5mm	0.0001 (0.01%)	4.9×10^{-1}	6.0×10^{-6}
	0.001 (0.1%)	4.9×10^{-1}	6.0×10^{-4}
	0.01 (1%)	4.8×10^{-1}	5.7×10^{-2}
500μm	0.0001 (0.01%)	4.8×10^{-1}	6.0×10^{-6}
	0.001 (0.1%)	4.8×10^{-1}	6.0×10^{-4}
	0.01 (1%)	4.7×10^{-1}	5.7×10^{-2}
50μm	0.0001 (0.01%)	4.4×10^{-1}	6.0×10^{-6}
	0.001 (0.1%)	4.4×10^{-1}	6.0×10^{-4}
	0.01 (1%)	4.3×10^{-1}	5.8×10^{-2}

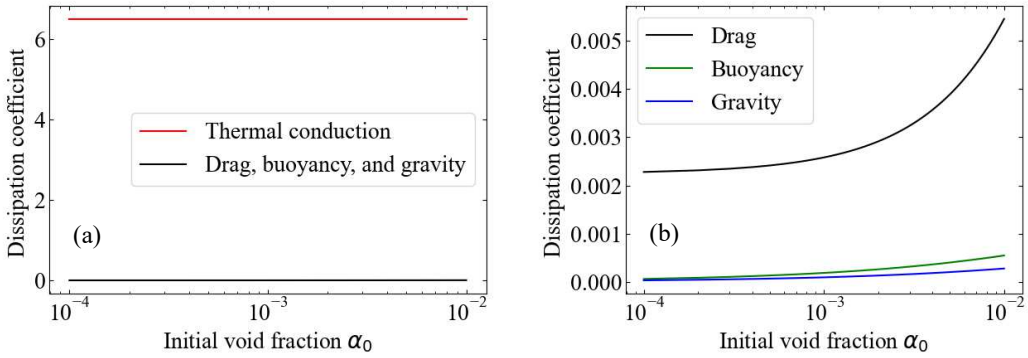

Figure 3: Comparison of the dissipation coefficients. (a) The red and black curves represent the coefficient owing to thermal conduction and sum of drag, buoyancy, and gravity, respectively. (b) The black, green, and blue curves represent the coefficient owing to drag, buoyancy, and gravity, respectively (Table 4). The calculation condition is the same as that in Fig. 2.

Table 4: Comparison of drag, buoyancy, and gravity in Fig. 3.

R_0^*	α_0	$\Pi_{4\mathrm{dr}}$	$\Pi_{4\mathrm{buo}}$	$\Pi_{4\mathrm{g}}$
5mm	0.0001 (0.01%)	7.4×10^{-5}	5.9×10^{-4}	2.9×10^{-4}
	0.001 (0.1%)	1.0×10^{-4}	1.9×10^{-3}	9.3×10^{-4}
	0.01 (1%)	4.0×10^{-4}	5.5×10^{-3}	2.8×10^{-3}
1mm	0.0001 (0.01%)	8.1×10^{-4}	1.2×10^{-4}	5.9×10^{-5}
	0.001 (0.1%)	9.6×10^{-4}	3.7×10^{-4}	1.8×10^{-4}
	0.01 (1%)	2.4×10^{-3}	1.1×10^{-3}	5.5×10^{-4}
500μm	0.0001 (0.01%)	2.3×10^{-3}	5.9×10^{-5}	2.9×10^{-5}
	0.001 (0.1%)	2.6×10^{-3}	1.8×10^{-4}	9.2×10^{-5}
	0.01 (1%)	5.5×10^{-3}	5.4×10^{-4}	2.8×10^{-4}
50μm	0.0001 (0.01%)	7.1×10^{-2}	5.7×10^{-6}	2.8×10^{-6}
	0.001 (0.1%)	7.4×10^{-2}	1.8×10^{-5}	8.9×10^{-6}
	0.01 (1%)	1.0×10^{-1}	5.3×10^{-5}	2.7×10^{-5}
10μm	0.0001 (0.01%)	7.1×10^{-1}	1.0×10^{-6}	5.2×10^{-7}
	0.001 (0.1%)	7.3×10^{-1}	3.2×10^{-6}	1.6×10^{-6}
	0.01 (1%)	8.5×10^{-1}	9.6×10^{-6}	4.9×10^{-6}

where f is the first-order perturbation of the nondimensional bubble radius. The constant coefficients are expressed as

$$\Pi_0 = \frac{1-\alpha_0}{6\alpha_0} V^2 v_{\mathrm{p}} \left[3p_{\mathrm{G0}}(\gamma_{\mathrm{e}} - \kappa) - \frac{\Delta^2}{\Omega^2} \right], \tag{62}$$

$$\Pi_1 = \frac{1}{6} \left[k_1 + \frac{u_0 - (1-\alpha_0)v_p}{\alpha_0(1-\alpha_0)v_p} k_2 + \frac{1-\alpha_0+\beta_1}{(1-\alpha_0)\beta_1 v_p} k_3 + \frac{k_4}{\alpha_0(1-\alpha_0)v_p} + \frac{\beta_1 + \alpha_0 B}{\alpha_0 \beta_1 v_p} k_5 + \frac{p_{G0}[\alpha_0(1-\alpha_0) + \beta_1 + \alpha_0 B(1-\alpha_0)]}{\alpha_0 \beta_1 (1-\alpha_0) v_p^2} k_6 \right] < 0, \tag{63}$$

$$\begin{cases} k_1 = 6v_{\mathrm{p}}(2 - s_1) + 2s_2(3 - s_1), \\ k_2 = -2\alpha_0 s_1 s_3, \\ \hat{k} = (\beta_1 + \beta_2)s_1(s_2 - s_3)v_{\mathrm{p}} - \beta_1(s_2^2 - s_3^2) - Bs_1 s_4, \\ k_3 = p_{\mathrm{G0}} s_1(3 - s_5) + 6p_{\mathrm{G0}}(s_5 - 2) + \hat{k}, \\ k_4 = -\alpha_0 \hat{k} + \alpha_0 s_1 s_4 - 2(1-\alpha_0)s_3^2 - 2\alpha_0 s_1 s_3(v_{\mathrm{p}} - u_0), \\ k_5 = -6p_{\mathrm{G0}}(3\kappa - \gamma_{\mathrm{e}} - 1) - \frac{2\Delta^2}{\Omega^2} - \frac{1}{2}(s_2 - s_3)^2, \\ k_6 = -3v_{\mathrm{p}}(3\kappa^2 - 5\kappa + 2), \end{cases} \tag{64}$$

$$\Pi_2 = \frac{\beta_1 + \alpha_0 B}{6\alpha_0 \beta_1} V \Delta \left[3p_{G0}(\gamma_e - \kappa) - \frac{\Delta^2}{\Omega^2} \right] < 0, \tag{65}$$

$$\Pi_3 = \frac{\beta_1 + \alpha_0 B}{6\alpha_0 \beta_1} \Delta^2 v_p > 0, \tag{66}$$

$$\Pi_4 = \Pi_{4\mathrm{buo}} + \Pi_{4\mathrm{gr}} + \Pi_{4\mathrm{dr}} + \Pi_{4\mathrm{th}} > 0, \tag{67}$$

$$\Pi_{4\mathrm{buo}} = \frac{s_1 g}{6\beta_1 v_{\mathrm{p}}} > 0, \tag{68}$$

$$\Pi_{4\mathrm{gr}} = \frac{s_1 g}{6(1-\alpha_0)v_{\mathrm{p}}} > 0, \tag{69}$$

$$\Pi_{4\mathrm{dr}} = \frac{A\mu_{\mathrm{L}}}{32 v_{\mathrm{p}} \beta_1 \Delta^2}(s_3 - s_2) > 0, \tag{70}$$

$$\Pi_{4\mathrm{th}} = \frac{p_{\mathrm{G0}}[\alpha_0(1-\alpha_0) + \beta_1 + \alpha_0 B(1-\alpha_0)]}{2\alpha_0 \beta_1 (1-\alpha_0) v_{\mathrm{p}}^2}(\kappa - 1)\zeta_{\mathrm{STM1}} > 0. \tag{71}$$

where Π_0 is the advection coefficient, Π_1 is a nonlinear coefficient, Π_2 and Π_4 are the dissipation coefficients, and Π_3 is the dispersion coefficient. Π_2, $\Pi_{4\mathrm{buo}}$, $\Pi_{4\mathrm{gr}}$, $\Pi_{4\mathrm{dr}}$, and $\Pi_{4\mathrm{th}}$ are the dissipation coefficients owing to acoustic radiation, buoyancy, gravity, drag, and thermal conduction, respectively. In this way, the total attenuation of waves is divided into independent attenuation components due to various forces based on a theoretical method.

3.3 Discussion

The relationship between the Bjerknes force and coefficients is shown in Fig. 2, Table 2, and Table 3. The absolute values of nonlinear, dissipation, and dispersion coefficients increased owing to Bjerknes force. In particular, the effect of Bjerknes force on Π_4 is significant. A comparison of the dissipation coefficients Π_4 is shown in Fig. 3 and Table 4. The dissipation effect of thermal conduction was the largest, followed by those of drag, buoyancy, and gravity. As this result depends on the temperature gradient model [82], the influence of thermal conduction on the waves may be overestimated.

The dissipation term owing to acoustic radiation ($\Pi_2 \partial^2 f / \partial \xi^2$) has a different mechanism from that owing to drag, gravity, buoyancy, and thermal conduction ($\Pi_4 f$) with respect to the unknown variable. Therefore, we conducted a numerical analysis using the split-step Fourier method used in previous studies [59, 63, 84]. Our previous study [63] indicated that the dissipation effect of the thermal conduction was the largest, followed by those of acoustic radiation and drag force obtained from the numerical analysis. Figure 4 illustrates the temporal evolution of the numerical solutions to the KdVB equation. The black, blue, and red curves represent waveforms with only acoustic radiation, with drag, gravity, and buoyancy forces and with only thermal conduction, respectively. We assume that the initial

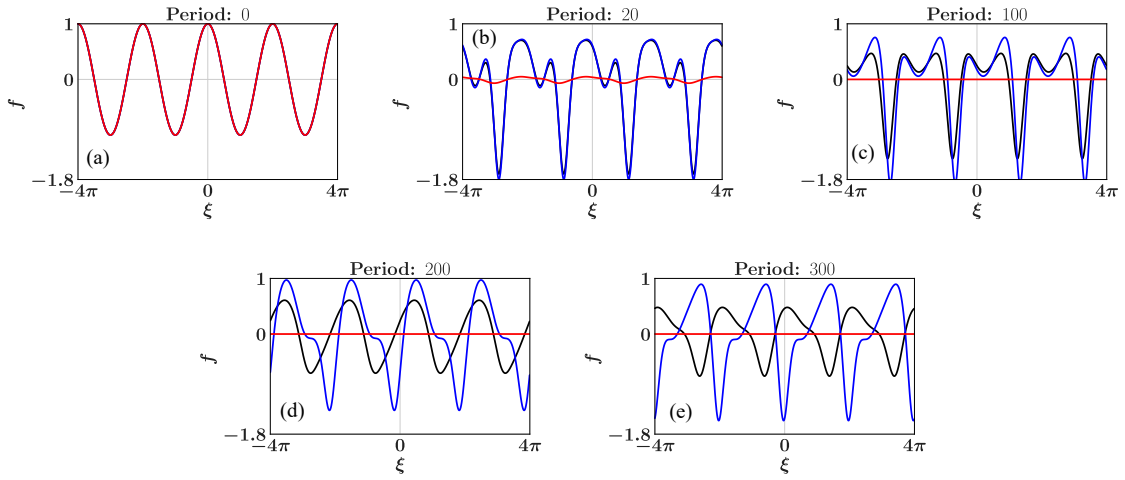

Figure 4: The numerical solution of the KdVB equation is presented for $\alpha_0 = 0.001$ and $R_0^* = 500\mu\mathrm{m}$. The horizontal axis represents the nondimensional space coordinate ξ, while the vertical axis shows the first-order perturbation of the nondimensional bubble radius f. The periods evaluated are (a) 0, (b) 20, (c) 100, (d) 200, and (e) 300. Waveforms are depicted in black, blue, and red to indicate the effects of acoustic radiation, the combined forces of drag, gravity, and buoyancy, and thermal conduction, respectively. The computational parameters, consistent with those in Fig. 2, include grid steps of 1024, a numerical integration time duration of 0.001, and a computational domain size of 8π.

waveform of the solution is a cosine wave. The dissipation effect of thermal conduction was the largest, followed by those of acoustic radiation, drag, buoyancy, and gravity. This order was effective in the range from $R_0^* = 50\mu\mathrm{m}$ to $1\mathrm{mm}$. As shown in Table 4, the larger the initial bubble radius R_0^*, the smaller the damping effect of drag $\Pi_{4\mathrm{dr}}$. At $R_0^* = 5\mathrm{mm}$, the damping effect of drag was smaller than that of gravity. At $R_0^* = 10\mu\mathrm{m}$, the damping effect of drag was larger than that of acoustic radiation.

4 Conclusions

Previous studies have not clarified the relationship between the forces acting on bubbles and waves in bubbly flows. Although the validity of ignoring forces acting on the bubble has not been demonstrated, previous theoretical studies on nonlinear pressure waves in bubbly flows did not incorporate these forces. In this study, we theoretically examined the weak nonlinear propagation of plane (one-dimensional) pressure progressive waves in water flows containing spherical bubbles, particularly focusing on the effects of gravity, buoyancy, and Bjerknes forces acting on bubbles. Using the method of multiple scales, the KdVB equation describing weakly nonlinear propagation of long waves with a low frequency was derived. The following findings were obtained:

(i) The Bjerknes force acting on the bubbles contributed to the nonlinearity, dissipation, and dispersion of waves and increased the three effects.

(ii) The drag, gravity, and buoyancy forces acting on the bubbles contributed to dissipation and increased the value of the dissipation coefficients.

(iii) In the range from $R_0^* = 50\mu\mathrm{m}$ to $1\mathrm{mm}$, the dissipation effect decreased in the order: thermal conduction, acoustic radiation, drag, buoyancy, and gravity.

This study revealed that the attenuation of waves owing to the forces acting on gas bubbles is quantitatively small. This is the first study to demonstrate the validity of ignoring forces for pressure wave propagation in bubbly flows. In future research, the theoretical framework developed here will be applied to a cavitating flow in hydraulic machinery such as pump and water pipe. A lift could not be introduced here because this study considered only the one-dimensional case. The effect of forces such as lift [44, 45, 46] and buoyancy force on waves will be investigated in future research in the framework of multidimensional problem.

Acknowledgments

This study was funded by JSPS KAKENHI (22K03898), the JKA and its promotion funds from KEIRIN RACE, and the Komiya Research Grant from the Turbomachinery Society of Japan. This work was also based on results obtained from a project subsidized by the New Energy and Industrial Technology Development Organization (NEDO) (JPNP20004). We thank the referees for their valuable comments, and Editage (www.editage.com) for English language editing.

Appendix

The inhomogeneous terms K_i $(1 \leq i \leq 6)$ in (51)–(56) are given by

$$K_1 = -\frac{\partial u_{\mathrm{G}1}}{\partial x_1} + \frac{\mathrm{D}}{\mathrm{D}t_1}(3R_1 - \alpha_1) + 3\frac{\mathrm{D}}{\mathrm{D}t_0}[R_1(\alpha_1 - 2R_1)] + \frac{\partial}{\partial x_0}[u_{\mathrm{G}1}(3R_1 - \alpha_1)], \tag{A.1}$$

$$K_2 = (1-\alpha_0)\frac{\partial u_{\mathrm{L}1}}{\partial x_1} - \alpha_0\frac{\mathrm{D}\alpha_1}{\mathrm{D}t_1} - \alpha_0\frac{\partial}{\partial x_0}(\alpha_1 u_{\mathrm{L}1}) + (1-\alpha_0)\frac{\mathrm{D}\rho_{\mathrm{L}1}}{\mathrm{D}t_0}, \tag{A.2}$$

$$K_3 = p_{\mathrm{G}0}\frac{\partial}{\partial x_1}(3R_1 - T_{\mathrm{G}1}) + p_{\mathrm{G}0}\alpha_1\frac{\partial}{\partial x_0}(3R_1 - T_{\mathrm{G}1}) + 3p_{\mathrm{G}0}\frac{\partial}{\partial x_0}[R_1(T_{\mathrm{G}1} - 2R_1)] + K_{\mathrm{F}}, \tag{A.3}$$

$$\begin{aligned} K_4 = {} & \frac{\mathrm{D}}{\mathrm{D}t_1}[u_0\alpha_0\alpha_1 - (1-\alpha_0)u_{\mathrm{L}1}] - (1-\alpha_0)\frac{\partial}{\partial x_1}(p_{\mathrm{L}1} + u_0 u_{\mathrm{L}1}) + \alpha_0\frac{\mathrm{D}}{\mathrm{D}t_0}(\alpha_1 u_{\mathrm{L}1}) \\ & + u_0\alpha_0\frac{\partial}{\partial x_0}(\alpha_1 u_{\mathrm{L}1}) - (1-\alpha_0)\frac{\partial u_{\mathrm{L}1}^2}{\partial x_0} + \alpha_0\alpha_1\frac{\partial p_{\mathrm{L}1}}{\partial x_0} - \alpha_0 K_{\mathrm{F}} - (1-\alpha_0)u_0\frac{\mathrm{D}\rho_{\mathrm{L}1}}{\mathrm{D}t_0} \\ & - \alpha_0\left\{\left[3(\gamma_{\mathrm{e}} - 1)p_{\mathrm{G}0} - \frac{\Delta^2}{\Omega^2}\right]R_1 + p_{\mathrm{G}0}T_{\mathrm{G}1} - p_{\mathrm{L}1}\right\}\frac{\partial \alpha_1}{\partial x_0} + g\alpha_0\alpha_1, \end{aligned} \tag{A.4}$$

$$K_5 = \Delta^2\frac{\mathrm{D}^2 R_1}{\mathrm{D}t_0^2} - V\Delta\frac{\mathrm{D}p_{\mathrm{L}1}}{\mathrm{D}t_0} + 3p_{\mathrm{G}0}R_1T_{\mathrm{G}1} - \left[3(2-\gamma_{\mathrm{e}})p_{\mathrm{G}0} + \frac{\Delta^2}{\Omega^2}\right]R_1^2 - \frac{1}{4}(u_{\mathrm{G}1} - u_{\mathrm{L}1})^2, \tag{A.5}$$

$$K_6 = -3\frac{\mathrm{D}}{\mathrm{D}t_0}\left[(\kappa - 1)T_{\mathrm{G}1}R_1 + \frac{1}{2}(\kappa - 1)(3\kappa - 4)R_1^2\right] - \zeta_{\mathrm{STM}1}T_{\mathrm{G}1}, \tag{A.6}$$

where

$$\frac{\mathrm{D}}{\mathrm{D}t_1} = \frac{\partial}{\partial t_1} + u_0\frac{\partial}{\partial x_1}, \tag{A.7}$$

$$\begin{aligned} K_{\mathrm{F}} = {} & -\beta_1\frac{\mathrm{D}}{\mathrm{D}t_1}(u_{\mathrm{G}1} - u_{\mathrm{L}1}) - \beta_1\alpha_1\frac{\mathrm{D}}{\mathrm{D}t_0}(u_{\mathrm{G}1} - u_{\mathrm{L}1}) - \beta_1\left(u_{\mathrm{G}1}\frac{\partial u_{\mathrm{G}1}}{\partial x_0} - u_{\mathrm{L}1}\frac{\partial u_{\mathrm{L}1}}{\partial x_0}\right) \\ & - \beta_2(u_{\mathrm{G}1} - u_{\mathrm{L}1})\frac{\mathrm{D}\alpha_1}{\mathrm{D}t_0} - \frac{3A\mu_{\mathrm{L}}}{16\Delta^2}(u_{\mathrm{G}1} - u_{\mathrm{L}1}) + \alpha_1 g - B\left(\frac{\partial p_{\mathrm{L}1}}{\partial x_1} + \alpha_1\frac{\partial p_{\mathrm{L}1}}{\partial x_0}\right). \end{aligned} \tag{A.8}$$

Author Declarations
Conflict of Interest

The authors have no conflicts to disclose.

Author Contributions

S.A. and T.K. contributed equally to this work.

Data availability

The data supporting the findings of this study are available from the corresponding author upon reasonable request.